Analysis and Optimization of the Control System of a Hydraulic Fine-Blanking Press

Mmse Journal Hotmail, Guodong Yi, Peng Zhang

Analysis and Optimization of the Control System of a Hydraulic Fine-Blanking Press

Guodong Yi[1, a], Peng Zhang[1]

1 – School of Mechanical Engineering, Zhejiang University, Hangzhou, China

a – ygd@zju.edu.cn

DOI **10.2412/mmse.39.87.164** provided by Seo4U.link

Keywords: hydraulic fine-blanking press, open-loop control, closed-loop control, optimization, simulation.

ABSTRACT. Fine-blanking is an efficient and precise machining method. The hydraulic control system of the fine-blanking press has an important influence on the forming efficiency and accuracy of the part. The paper puts forward an analysis and optimization methods of the control system for velocity stability. A hydraulic control system model is established and the main parameters of blanking process such as blanking force, blank holder force and counter force were calculated and analyzed. According to the velocity changes of the master cylinder with open-loop control in blanking process, the causes and effects of each change point and the variation characteristics of load, acceleration and displacement of master cylinder are elaborated. The velocity changes with closed-loop control based on velocity and position feedback are described and compared with that of the open-loop control. Based on the comparative analysis, the influences of the system and components on the velocity are studied, and the open-loop control is selected as the control method of the fine-blanking press. The optimal control strategy for the steady velocity of main cylinder is proposed with the automatic optimization algorithm and the simulation results.

Introduction. Fine-blanking is a high efficiency and high-precision machining method, which has been widely used because the blanking parts can be used directly without further processing. However, the precision of the repeatability of the precision is difficult to guarantee because the sharp blanking load and speed change rapidly in a short time. However, it is difficult to maintain the repeatability precision of the fine-blanking due to the tremendous changes in load and speed in a very short period of time. To solve this problem, it needs not only a high rigidity mechanical structure but also an effective hydraulic control system. The control system regulates and controls the pressure and flow of the hydraulic system to balance the load and stabilize the speed so that the fine blanking working conditions will not fluctuate violently. Therefore, it is conducive to stabilizing the operation of the fine-blanking press and improve the machining quality through the analysis and optimization of the control strategy [1].

A number of optimization methods have been proposed: Shen studied the optimal control variable trajectory under a given circle using the dynamic programming algorithm to reduce the fuel consumption clearly without deteriorating the performance [2]. Baghestan proposed a nonlinear back stepping control algorithm with an energy-saving approach for position tracking to satisfy the tracking and energy-saving objectives [3]. Ding proposed the approximate internal model control integrated with a position feedback control in cascade control design to improve the trajectory-tracking performance of the hydraulic servomechanism [4]. Coelho presented an adaptive cascade controller tuned by using evolutionary algorithms for performance optimization of the trajectory tracking control of a hydraulic actuator with an overlapped proportional valve [5]. Tri introduced a control algorithm, which is the combination of a modified back stepping control with an iterative learning mechanism for the adaptive trajectory tracking control of an electrohydraulic actuator [6].

PID (proportional-integral-derivative)-based methods are the most widely researched and applied: Jia established the cerebellar model articulation controller neural network and PID coupling control strategy to enhance the tracking performance of hydraulic roll bending loop [7]. Shen studied a PI controller combined with an offline designed feedback controller and an online adaptive compensator to improve force tracking performance of an electro-hydraulic force servo system [8]. Chalupa proposed an optimal PID and model predictive controllers for both a linearized model and the nonlinear system [9]. Ye presented an improved particle swarm optimization algorithm to search for the optimal PID controller gains for the nonlinear hydraulic system [10]. Li used trial and error to get suitable PID parameters for electro-hydraulic proportional control to ensure the accuracy of conveyor speed control [11]. Du proposed a new load-prediction based method using feed forward control for the servomotor and control valves to supplement conventional PI feedback control [12]. Elbayomy designed a PID controller optimized by the genetic algorithm to improve the performances of the hydraulic servo actuator system[13]. Muhammad presented an optimal hybrid fuzzy proportion integral derivative controller based on combination of PID and fuzzy controllers to acquire precise tracking performances [14]. Cao optimized PID Parameters of hydraulic system with NLPQL algorithm to obtain the global optimal solution effectively [15]. Zheng introduced a fuzzy PID control method based on the relationships between the PID parameters and the response characteristics to improve the overall performance of the electro-hydraulic position servo system [16].

Based on the above research, the paper establishes the hydraulic control system model of a fine-blanking machine calculates and analyzes the main blanking process parameters and their mutual relations. Then, the change characteristics of speed, load, acceleration and displacement of the master cylinder under open-loop control and closed-loop control are studied, and the control method suitable for fine blanking system is determined through comparative analysis. Finally, an optimal control strategy is set up based on the characteristics of fine blanking to meet the performance and quality requirements of the blanking process.

Hydraulic Control System Model of the Fine-blanking Press. The following assumptions are proposed in the modelling according to the characteristics of blanking process:

(1) The master cylinder, press cylinder and counter cylinder are the main objects, and the stepping cylinder is simplified due to its little influence on the punching.

(2) All solenoid directional valves are considered as logic elements, that is, the valves are opened and closed in full synchronism with the control signal.

(3) The hydraulic components that are not closely related to the blanking process are omitted.

(4) The influence of system oil leakage is not considered to improve the analysis simulation speed.

The hydraulic control system model is shown in Fig. 1.

Calculation of the fine-blanking Load. The fine-blanking forces include the cutting force F_S, the blank holder force F_R, and the counterforce F_G.

The cutting force F_S is a function of cutting length L, material tensile strength σ_b, thickness S, and the coefficient f_1:

$$F_S = L \cdot S \cdot \sigma_b \cdot f_1 \tag{1}$$

where f_1 – is determined by the Poisson's ratio; generally, f_1 = 0.9.

The blank holder force F_R is a function of blank holder circumference L_R and height h, material tensile strength σ_b, and the coefficient f_2:

$$F_R = L_R \cdot 2h \cdot \sigma_b \cdot f_2 \tag{2}$$

where f_2 = 1.9 while σ_b = 600 MPa.

The counterforce F_G is a function of compression area A and counterforce intensity p_G:

$$F_G = A \cdot p_G \tag{3}$$

where p_G = 70 MPa in the large area and 20 MPa in the small area.

The typical process parameters were designed based on the working conditions of the fine blanking press as follows: material thickness is 4 mm, cutting length is 1200 mm, material tensile strength is 600 MPa, blank holder height is 0.6 mm. F_S, F_R and F_G were calculated based on the above computational formulas and parameters as follows: $F_S = 2500\ kN$; $F_R = 1575\ kN$; $F_G = 700\ kN$.

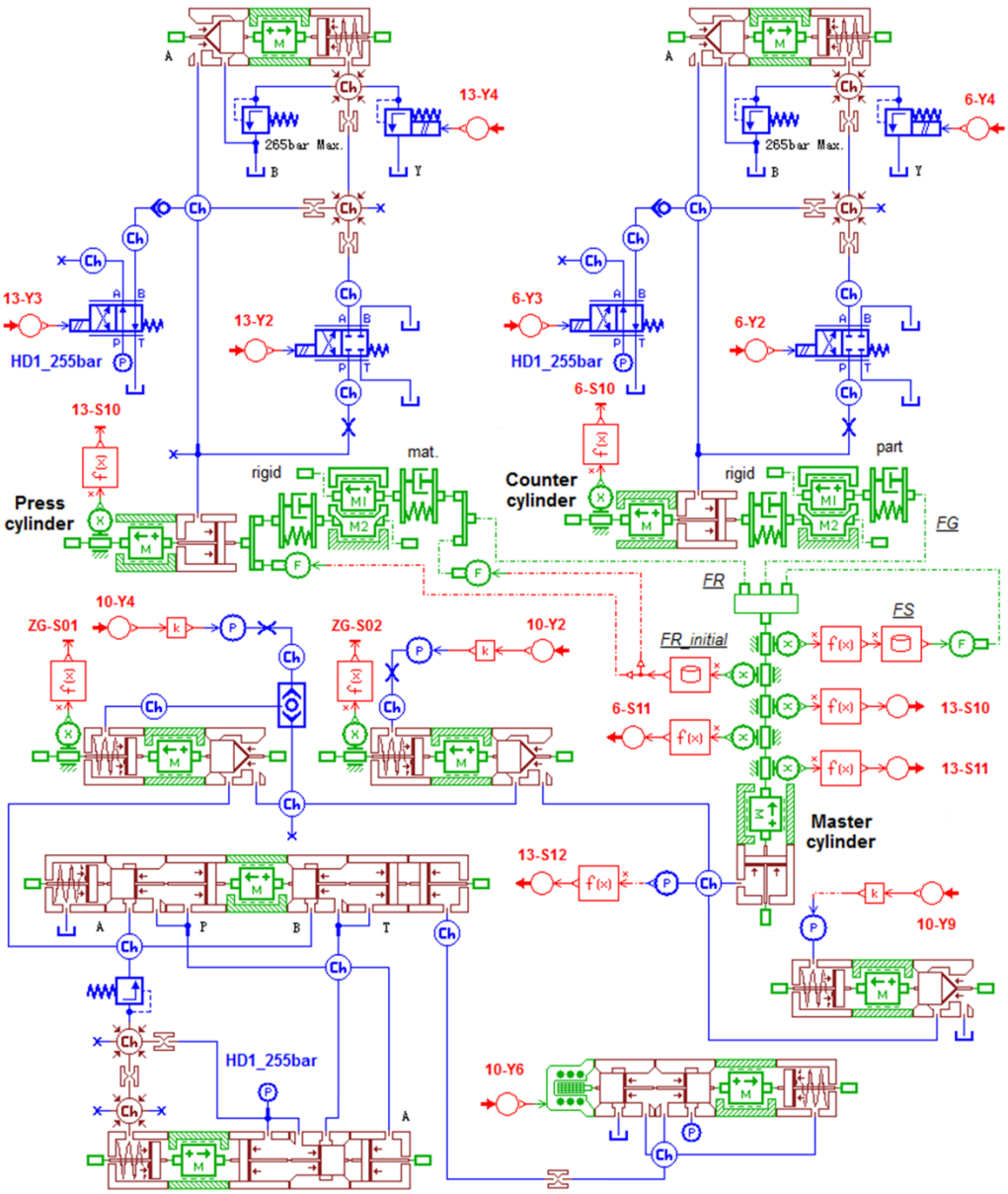

Fig. 1. The hydraulic control system model.

Relationship between the blank holder force and the pressing depth. The process of the blank holder pressing into the material is divided into two stages by the material elastic limit, the first one is elastic deformation, and the second stage is plastic deformation. The curve of blank holder force and pressing depth is shown in Fig. 2. After the blank holder is fully pressed into the material, the load of the master cylinder rises rapidly. At this time, the differential pressure switch 13-S12 is started and the pressure in the press cylinder is partially relieved, and the pressing process is completed.

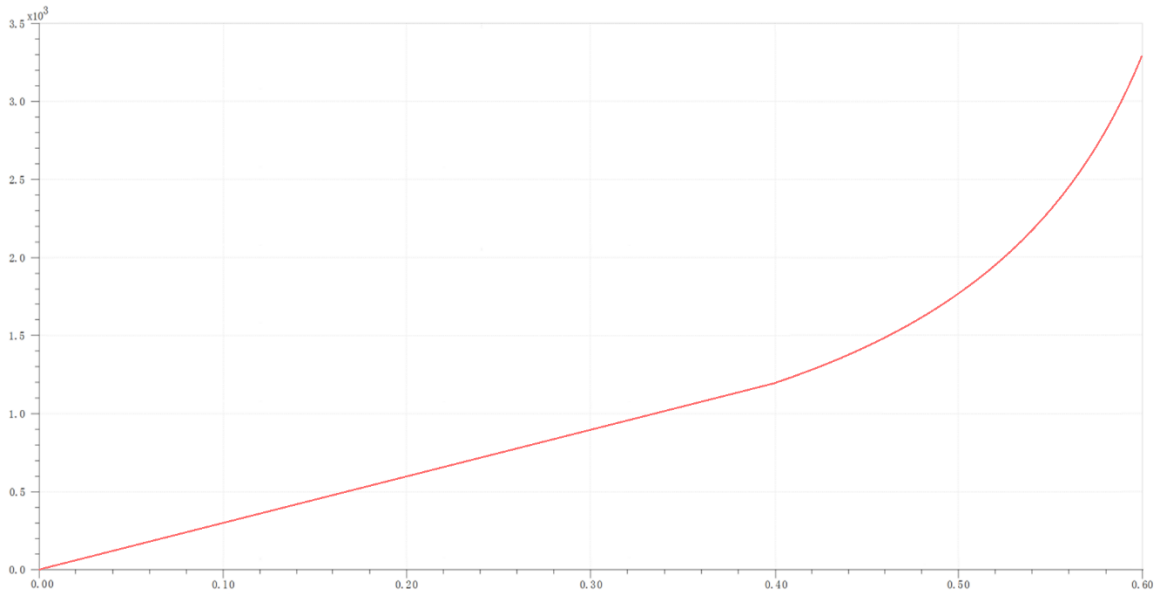

x: Pressing depth (mm); y: Blank holder force (kN).

Fig. 2. The curve of blank holder force and pressing depth.

The relationship between the blanking force and the blanking thickness. The blanking force F_S rises sharply at the beginning of the punching process. Although the deformation of the sheet decreases the shearing area, but F_S is increasing due to the hardening of the material until the peak is reached. Then, F_S starts to declined gradually due to the effect of the shear area reduction on the blanking force exceeds that of the material hardening, with the change trend similar to the extrusion process, and there is no sharp decline of the blanking force which often occurred in ordinary punching process due to the premature material fracture. In general, the limit of F_S appears at the position where the punching depth is about 1/3 of the plate thickness. The variation of the blanking force F_S with the blanking depth is shown in Fig. 3.

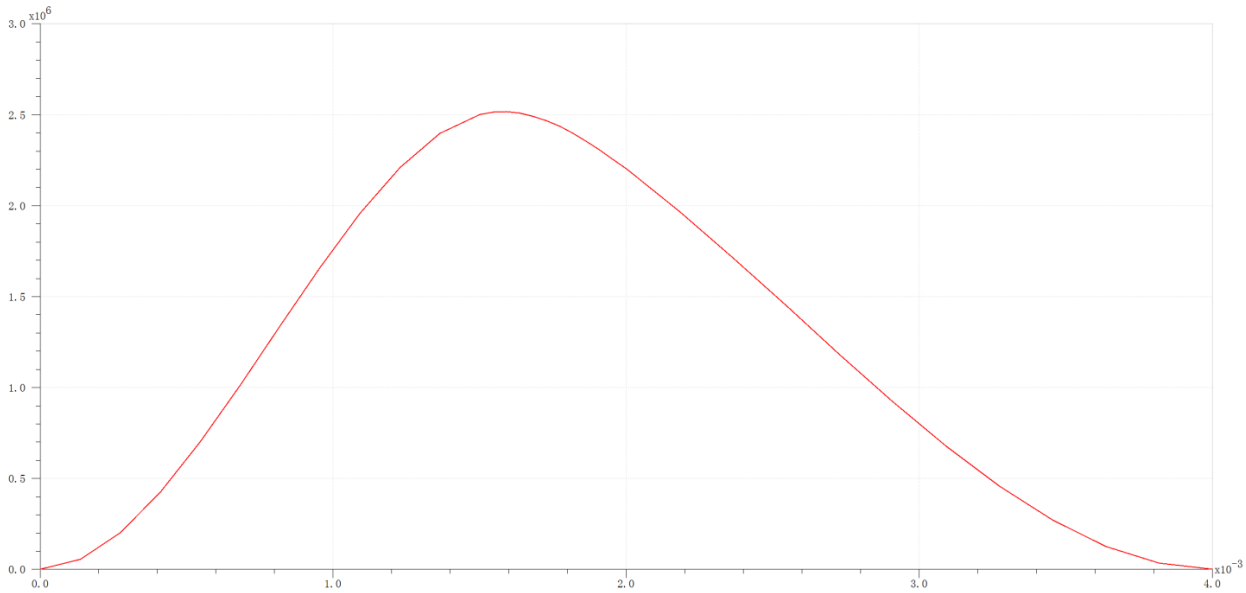

x: Blanking depth (m); y: Blank force (N).

Fig. 3. Variation of the blanking force with the blanking depth.

Analysis of the open-loop control. The purpose of analyzing the open-loop control process is to illustrate the operating status of the system at each stage of the blanking process and the relevant influencing factors, to clarify the inherent characteristics of the system.

The initial position of the punching start point is set to 0 and the start time is set to 0.2s. According to the hydraulic system model shown in Fig. 1, the action sequence of the main hydraulic elements during blanking process is shown in Fig. 4, and the velocity variation of the master cylinder in blanking process is simulated in Fig. 5.

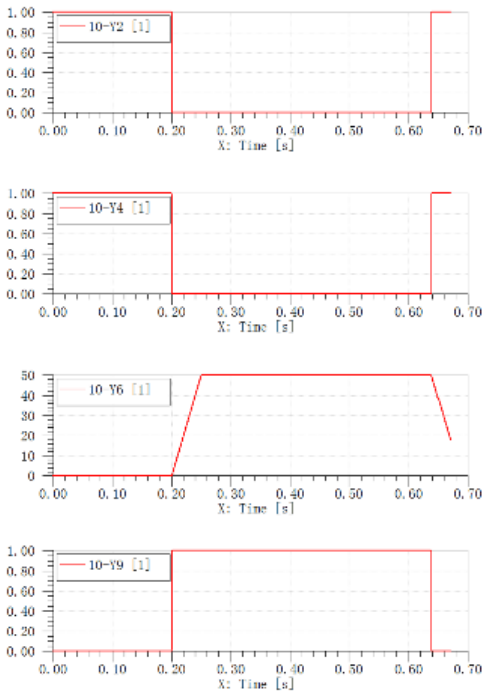

(a) Master cylinder

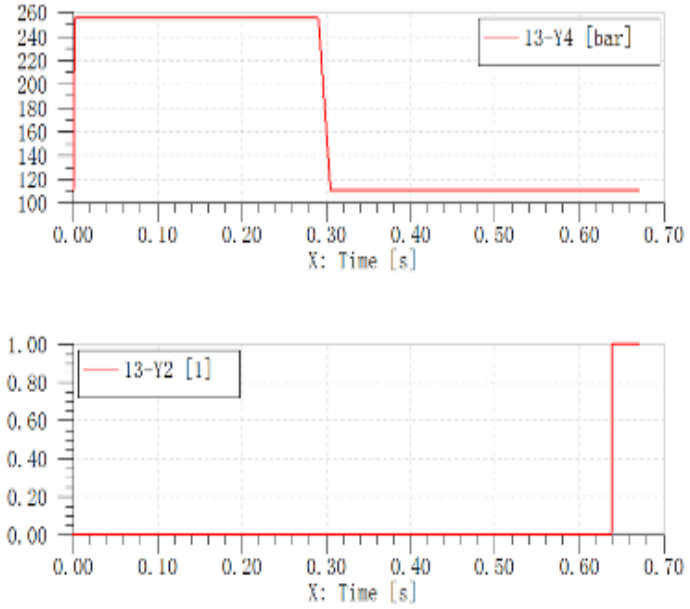

(b) Press cylinder

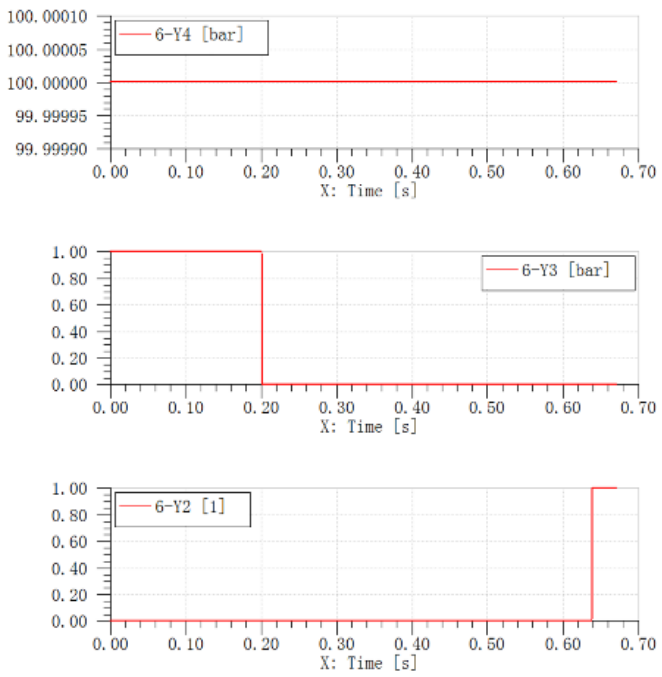

(c) Counter cylinder

Fig. 4. Action of the key valves in blanking process.

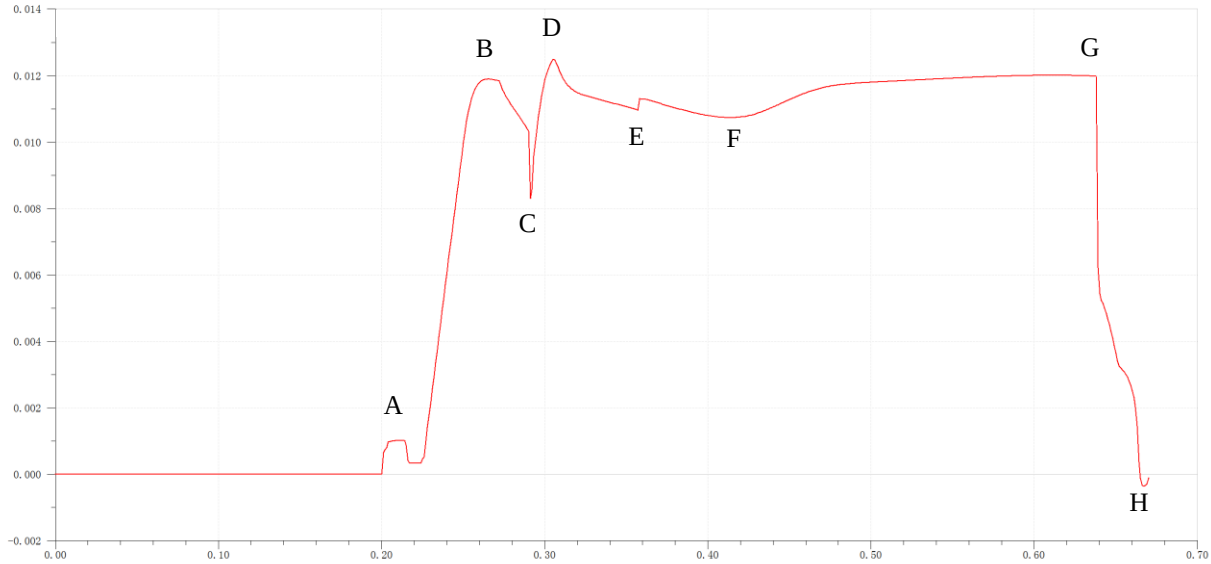

x: Time (s); y: Velocity of the master cylinder (m/s).

Fig. 5. Velocity variation curve of the master cylinder in open loop control.

The velocity of the master cylinder fluctuated during the blanking process, and the generation and influence of each velocity change point are as follows:

Velocity change point A:

A small peak of the velocity appears when the master cylinder starts, because the spool of the proportion valve has not yet started at this time, and the oil in the master cylinder is actually supplied by the relief valve on the control cover of the press regulating valve before the proportional valve.

When the cartridge valve on the main oil line just started, the large pressure difference between the two ends leads to the pressure inside the cylinder chamber close to 0 and the import pressure close to 245 bar, so the velocity rises rapidly in a short time. This process has a short duration of about 20 ms then the velocity reduces due to the throttling of the damping port. When the spool of the proportion valve started, the velocity rises again. The flow of the relief valve on the control cover of the press-regulating valve is shown in Fig. 6.

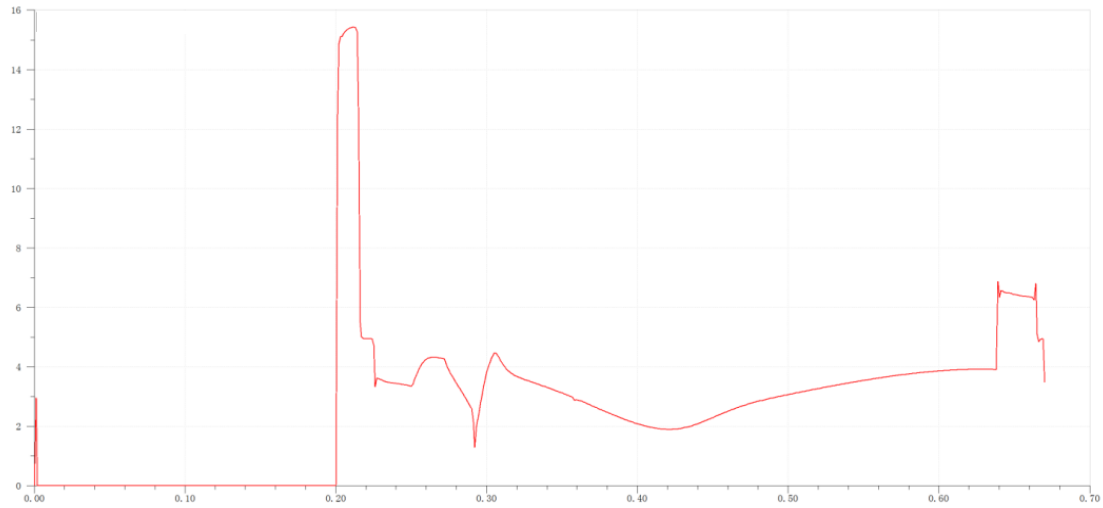

x: Time (s); y: flow of the relief valve on the control cover (L/min).

Fig. 6. The flow of the relief valve on the control cover of the press-regulating valve.

In Fig. 6, the flow through the relief valve in the first 20 ms is large, and then fluctuates at about 5 L/min according to the change of the master cylinder load to help the pressure relief valve to maintain the pressure stable at both ends of the proportional valve. After the proportional valve main spool started, the flow through the relief valve is relatively small and difficult to cause a large effect on the master cylinder velocity.

In practice, the speed change at point A will be smoother than the simulation results, because the solenoid directional valve that controls the cartridge valve on the main oil line is not started instantaneously, but cannot be eliminated completely in the given control mode.

Velocity change point B:

The velocity change point B appears at the end of the blank holder pressing process. Since the pressure cylinder has not yet started to retreat, the cylinder still maintains high pressure, and the master cylinder continues to rise, resulting in a rapid increase of the blank holder force. At the same time, the pressure difference between two ends of the proportional valve of the master cylinder begin to decline due to the response time of the pressure regulating valve, and the flow rate into the master cylinder is reduced with a certain opening width of the main spool of the proportional valve, resulting in a speed decrease after the point B.

Velocity change point C:

The velocity change point C appears when the mold is closed, at this time the blank holder force reach the maximum, and counterforce is also established, resulting in a peak of the main cylinder load, and a trough of speed, as shown in Fig. 7. The differential switch is started after the point C. The proportional relief valve of the press cylinder system is partially relieved, and the pressure-regulating cartridge raises the pressure of the proportional valve inlet, so the speed starts to rise again. The velocity change point C appears at the position where the master cylinder displacement is 0.605 mm with the set operating parameter, as shown in Fig. 8, the velocity change point 3 appears at the position where the master cylinder displacement is 0.605 mm.

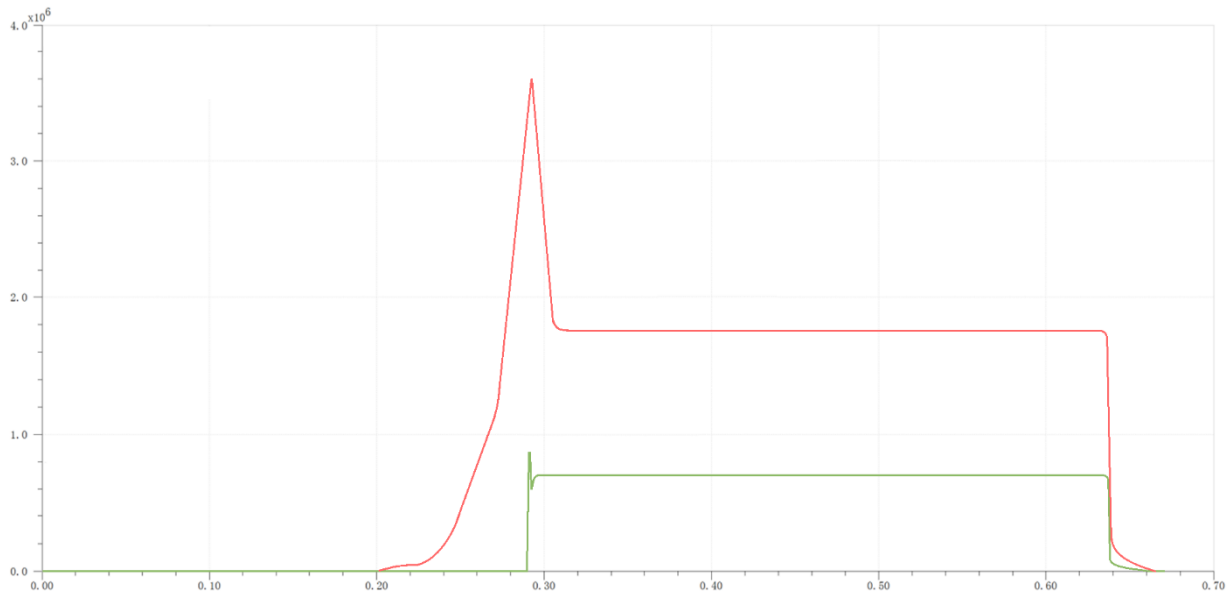

x: Time (s); y: Blank holder force (red) and counter force (green) (N).

Fig. 7. Curves of blank holder force and counter force.

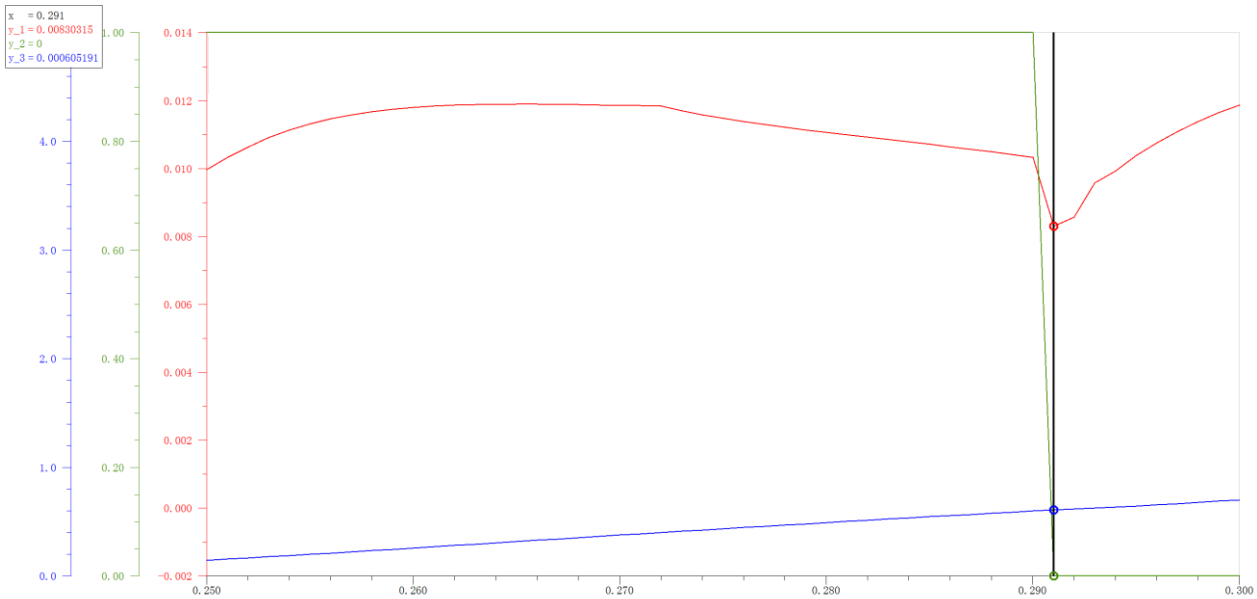

x: Time (s); y: Master cylinder velocity (red) (m/s), 13-S12 (green) (null), master cylinder displacement (blue) (m).

Fig. 8. Details of the velocity change point C.

The pressure variety of the solenoid pilot valve of the proportional relief valve is assumed to be synchronized with the control signal in the simulation, but there will be a delay in practice, resulting in the hysteresis of the pressure regulating of the press cylinder, and the rising cylinder may lead to plastic deformation of the material within the scope of the blank holder, which wastes energy and adversely affects the blanking process.

It is desirable that the pressure of the press cylinder begin to be partially relieved when the blank holder is fully pressed into the material and the press force required for the blanking process is established. The partial relief of the press cylinder pressure is controlled by the differential pressure switch 13-S12 or the position sensor 13-S10, ensuring that the blank holder can be fully pressed into the material.

If the counter force is established after the blank holder force is established, the calculated value of the diameter ratio of the two ends of the differential pressure switch is 1.4:1 according to the principle of force balance, which can be appropriately increased in practice due to the inertia of the system.

Velocity change point D:

The speed change point 4 appears at the beginning of the punching, at which point the pressure of the counter cylinder is partially relieved, and the blanking force is still small, so a trough of the master cylinder load appears. The pressure-regulating valve starts to raise the proportional valve inlet pressure according to the rise of the system pressure, but cannot immediately reach the target value due to the response time. The above factors lead to a speed overshoot at the speed change point D, as shown in Fig. 9.

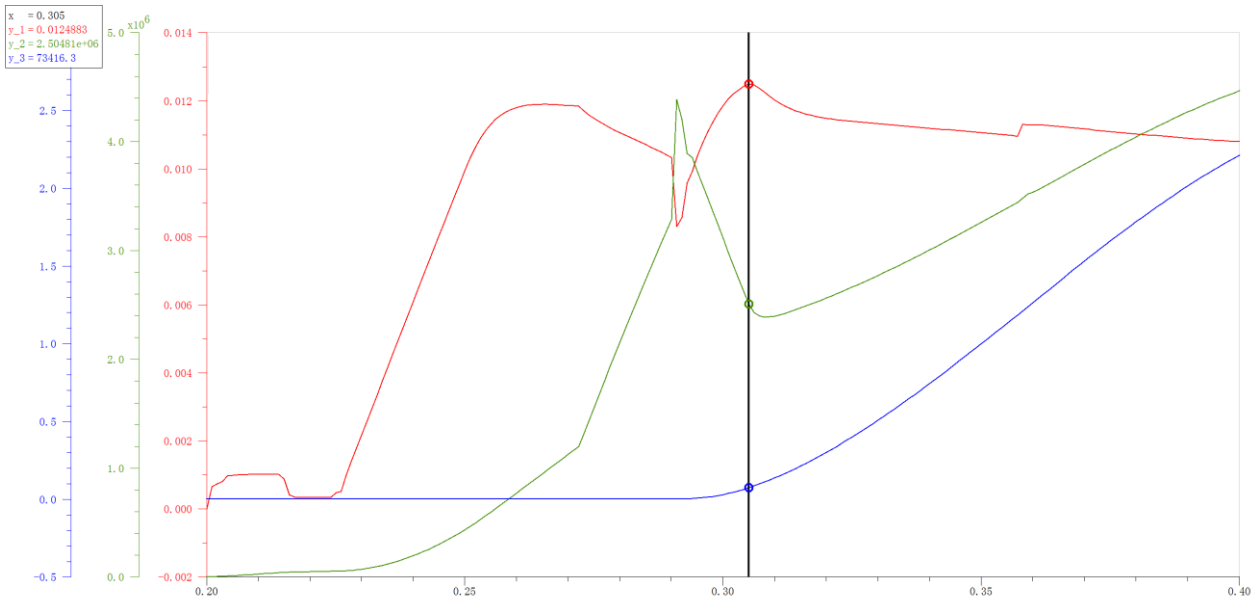

x: Time (s); y: Master cylinder velocity (red) (m/s), master cylinder load (green) (N), blanking force (blue) (N).

Fig. 9. Details of the speed change point D.

Velocity change point E:

The speed change at point *E* is due to a sudden change in the flow caused by the spool of the cartridge valve on the master cylinder oil circuit reaches the limit position. It takes about 160ms for the cartridge valve spool to be fully opened due to the throttling of the control chamber and a stroke of 12mm. During the opening process, a portion of the inlet flow is used to fill the cylinder chamber so that the outlet flow is less than the inlet flow. The inlet and outlet flow is equal after fully opening, resulting in a sudden increase in the speed at point 5, as shown in Fig. 10.

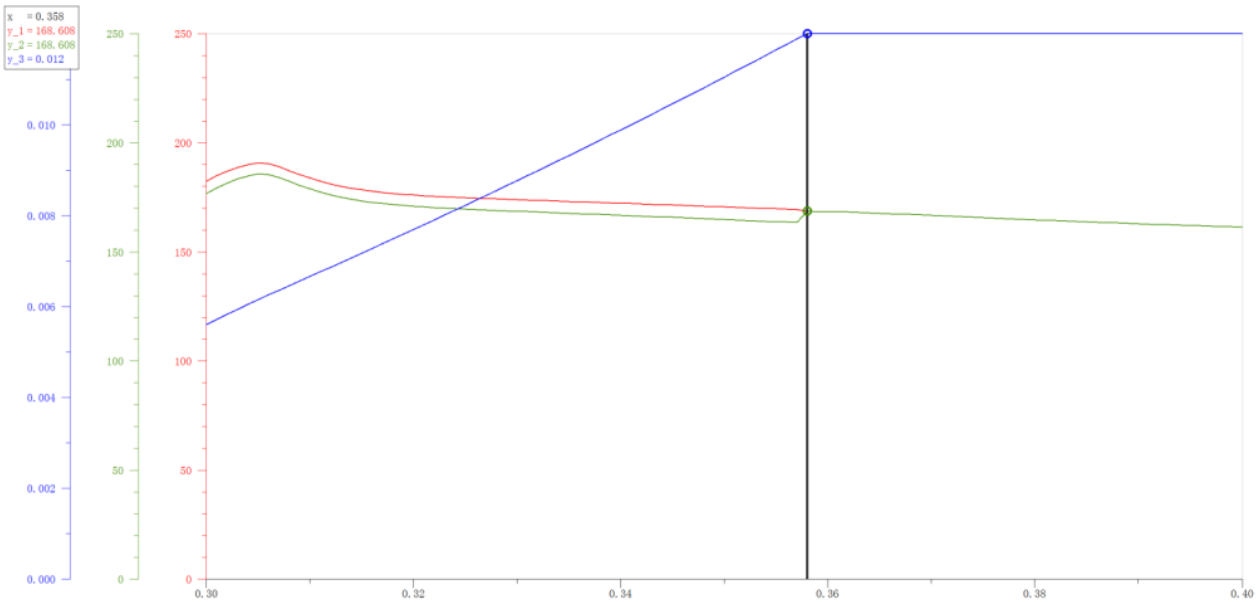

x: Time (s); y: Inlet flow (red) (L/min), outlet flow (green) (L/min), spool displacement (blue) (m).

Fig. 10. The impact of the opening size of the cartridge valve on the flow.

Velocity change point F:

A speed trough appears at point *F*, mainly because the peak of the master cylinder load appears at this time, but the speed changes slowly due to the slow change in the master cylinder load. The running state of each valve is stable at this stage, and the main factor affecting the speed change is the responsiveness of the pressure regulating cartridge valve on the system pressure changes, the faster the response speed is, of the master cylinder speed more stable. Due to the stability of the valve running state at this stage, the main factor affecting the speed change is the ability of the pressure regulating cartridge valve responding to the system pressure change, which means that the faster the response speed is, the more stable the master cylinder speed is.

Velocity change point G:

The speed change point G appears when the master cylinder reaches the preset vertex, and the spool of each valve of the master cylinder oil circuit is open at this moment. The main reason for the rapid decline in speed is the power off of the 10-Y9, resulting in the oil flowing to the master cylinder flows back to the tank through the cartridge valve controlled by 10-Y9.

At the power-on moment of the 10-Y9, the pressure of the counter cylinder and the pressing cylinder still exist, and the pressure of the master cylinder is large, resulting in a large flow back to the tank through the cartridge valve. Subsequently, the differential pressure between the master cylinder and the tank is reduced due to the pressure relief of the counter cylinder and the press cylinder, and the spool of the master cylinder oil circuit is gradually closed, resulting in a decrease in the flow of the return tank.

Velocity change point *H*:

At the speed change point *H*, all the valves on the master cylinder main oil circuit are closed, and the pressure of the counter cylinder and the press cylinder are relieved, so the elastic deformation of the material is recovered, resulting in a small displacement of the main cylinder after the speed rises to the highest point, and the speed becomes negative.

During the blanking process, the master cylinder load is the sum of the blank holder force, the counter force and the blanking force, as shown in Fig. 11.

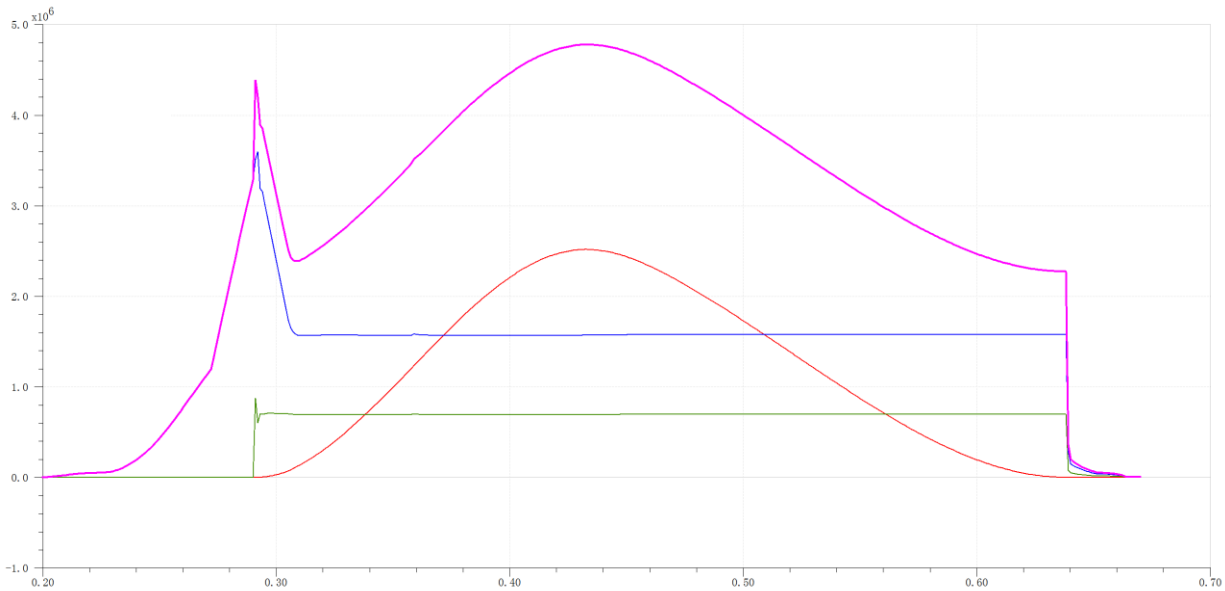

x: Time (s); y: Cutting force (red) (N), counter force (green) (N), blank holder force (blue) (N), total load of the master cylinder (magenta) (N).

Fig. 11. Load variation curve during blanking.

The peak 1 appears when the mold is closed, the peak 2 appears when the punching force is maximum, which is slightly lower than the peak 2.

The operating curve of the master cylinder in open-loop control mode is shown in Fig. 12.

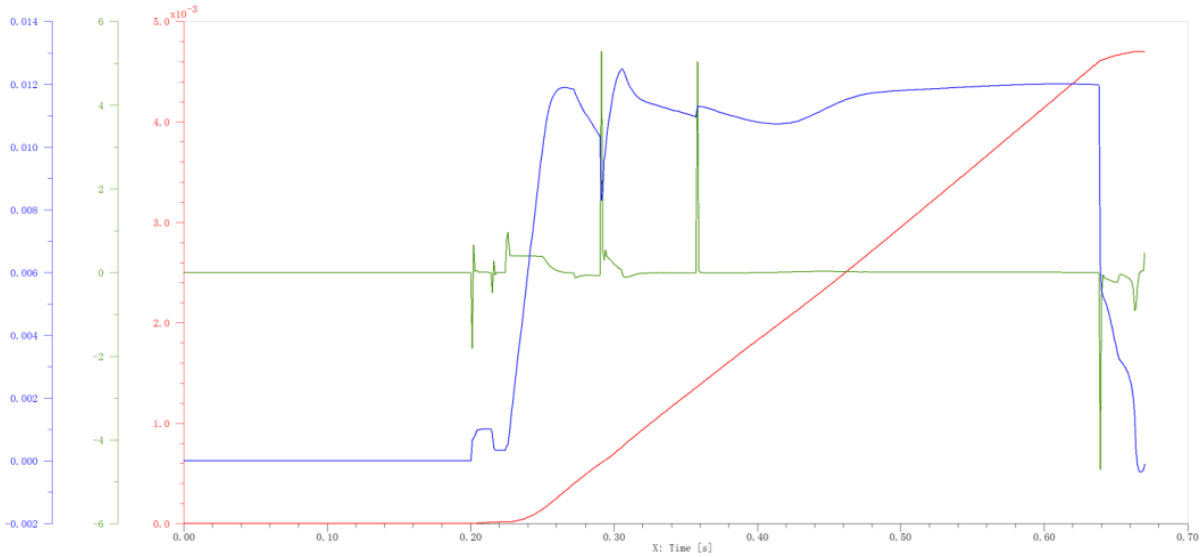

x: Time (s); y: Master cylinder displacement (red) (m), master cylinder acceleration (green) (m/s^2), master cylinder velocity (blue) (m/s).

Fig. 12. Operating curve of the master cylinder in open-loop control mode.

The displacement of the master cylinder during the blanking process is approximately straight, and the acceleration at each speed change point is less than 5 m/s^2.

Analysis of closed-loop control. The closed-loop control of the speed and position of the master cylinder is carried out to investigate the performance of the system.

With the slider speed as the control variable, the schematic diagram of the closed-loop control system is shown in Fig. 13 (a).

With the slider displacement as the control variable, the schematic diagram of the closed-loop control system is shown in Fig. 13 (b).

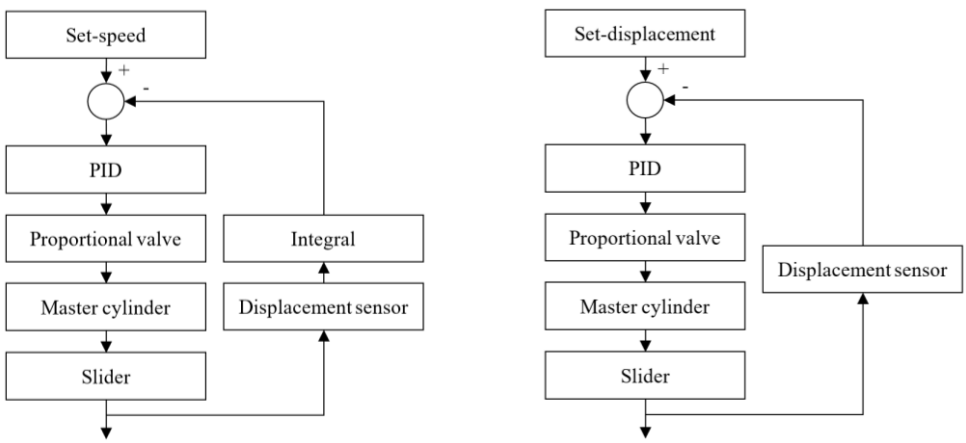

(a) Closed-loop control with speed (b) Closed-loop control with displacement

Fig. 13. Closed-loop control system.

The slider speed is simulated in a closed-loop control in the case where the proportional valve responds quickly (bandwidth is nearly 100 Hz), and the results are shown in Fig. 14.

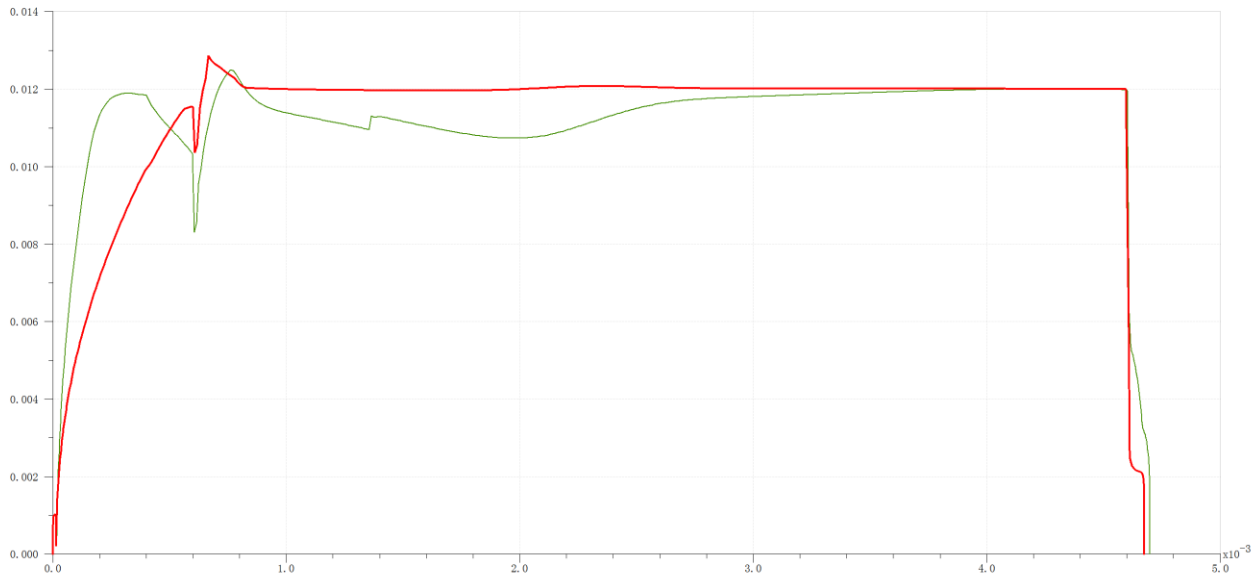

x: Slider displacement (m); y: Slider velocity in open-loop control (green) (m/s), slider velocity in closed-loop control (red) (m/s).

Fig. 14. Simulation of the speed in open loop and closed-loop control.

The speed variation in the open-loop control is suppressed by the closed-loop control of the speed, and the speed waveform of the system during the whole blanking process is also improved.The speed decline reduced by nearly 2/3 at position 1, but a short-time speed overshoot appears at position 2; In particular, the corresponding mold at the A has just closed the position, the speed of the decline reduced by nearly 2/3, but at the same time B appeared a short time speed overshoot; The speed fluctuation due to the fully open of the cartridge valve spool at position 3 is advanced to a displacement of 0.66mm, which is helpful to stabilize the speed in the blanking process; A small bump at position 4 is formed since the speed trough caused by the load crest is suppressed.

The simulation of the slider displacement in a closed-loop control is shown in Fig. 15.

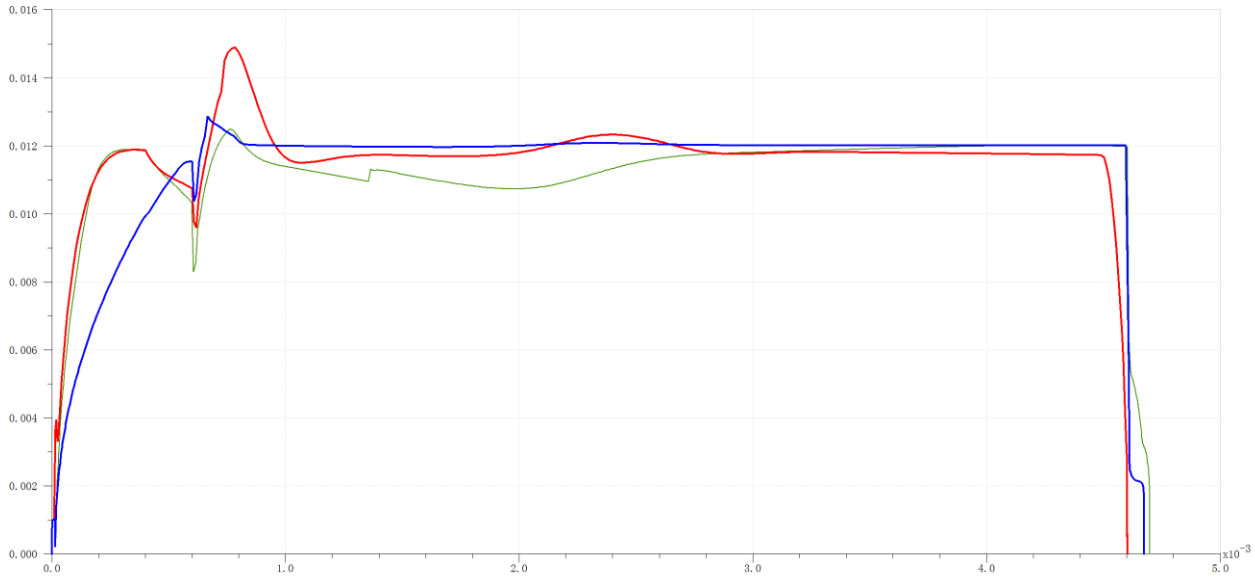

x: Slider displacement (m); y: Slider velocity in open-loop control (green) (m/s), slider velocity in closed-loop control of the displacement (red) (m/s) , slider velocity in closed-loop control of the speed (blue) (m/s).

Fig. 15. Simulation of the displacement in closed-loop control.

The speed appears a peak at position 1 by the displacement closed-loop control. The control accuracy of the displacement is improved and the slider can be stopped more accurately at position 2, but the fluctuation of the velocity curve is greater than that of the speed closed-loop control.

Comparison of the open/closed loop control. The main factor that affects the performance of the open-loop control is the response of the pressure regulating valve in front of the master cylinder proportional valve to the system pressure variation. The pressure-regulating valve adjusts the pressure difference between the two ends of the proportional valve to stabilize the flow into the master cylinder. The response time of the ideal pressure regulating valve is zero, that is, the outlet pressure of the proportional valve can be adjusted in real time according to the inlet pressure. In the open loop control simulation with the ideal pressure regulating valve, the slider speed is approximately straight, as shown in Fig. 16. Therefore, if the valve performance is better, the system speed can be stabilized by open loop control.

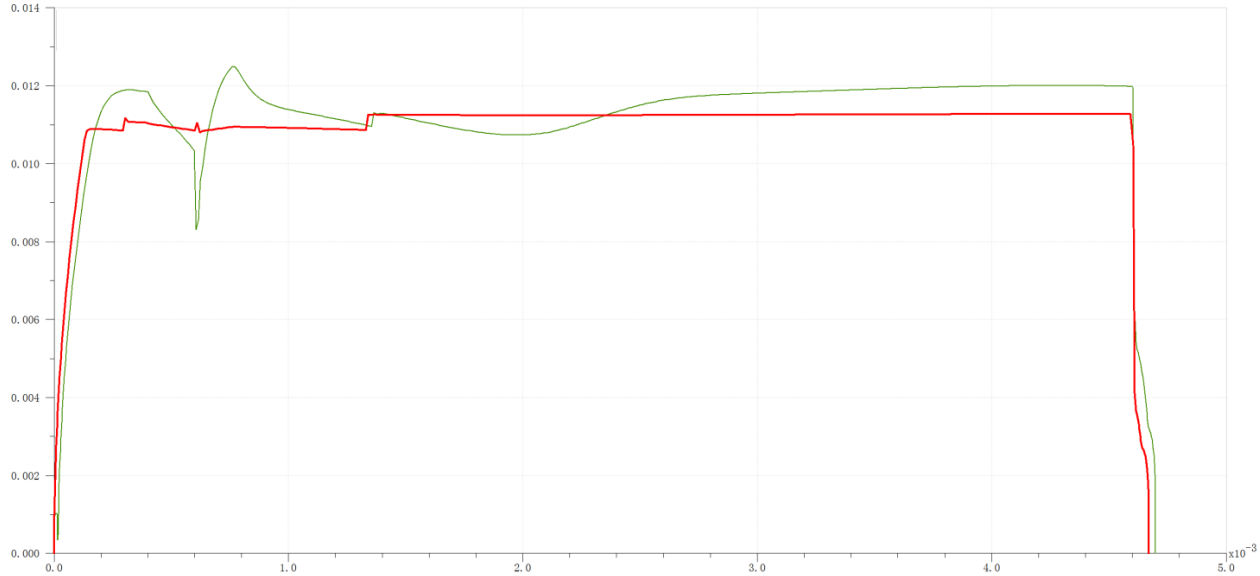

x: Slider displacement (m); y: Actual velocity of the slider (green) (m/s), ideal velocity of the slider (red) (m/s).

Fig. 16. Comparison of the slider speed.

The simulation results show that there is a risk of system oscillation due to the speed control of the proportional valve with low frequency response. The duration of the punching process is very short, usually less than 0.5 s, and the response time of the proportional valve is close to 0.1 s in the step change from 0.1 to 100 %, so the speed closed-loop control is not necessary. The slider displacement curves of the open loop control and the closed loop control are both close to the straight line due to the short stroke, as shown in Fig. 17.

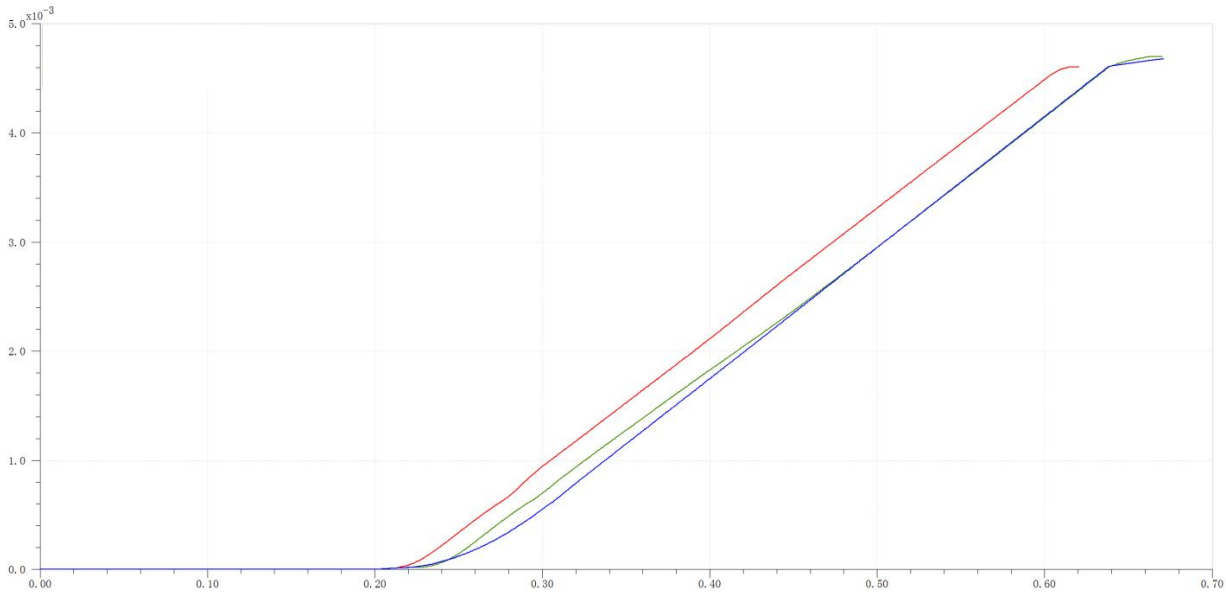

x: Time (s); y: Slider displacement in closed-loop control of displacement (red) (m), slider displacement in open-loop control (green) (m/s), slider displacement in closed-loop control of velocity (blue) (m/s).

Fig. 17. Displacement curve of the master cylinder in different control modes.

In summary, according to the variation in load and the configuration of the hydraulic system, the open-loop control mode should be adopted for the system during the blanking stage.

Optimization control strategy of the blanking process. The optimization control strategy is to adjust the system components according to the trend of slider speed and displacement variation in the open-loop control mode described in the previous section to reduce the speed fluctuation of the system.

The improvement of the cutting speed can accelerate the plastic deformation of the metal, which is conducive to the formation of smooth shear section, but will increase the die wear, and reduce its service life quickly. In the shearing process, the work of the punching force is converted into heat energy, most of which occurs in the shear zone of grain deformation. In the shearing process, the work of the punching force is converted into heat mainly in the grain deformation of the shear zone. The curve of the blanking force variety shows that most of the heat is generated in the first half of the shear process, so the appropriate reduction of the punching speed at this stage is helpful in improving the life of the die edge and stabilizing the quality of the shear section. The punching speed can be appropriately increased in the subsequent intermediate stage of the punching process to improve the punching efficiency.

The master cylinder speed should be reduced when the punching process approaches the end to control the position accuracy of the top dead center of the slider. When the slider is near the top dead center position, the opening of the proportional valve is small or is actually closed, the flow required for the last displacement to the top dead center (tens of microns) is together provided by the relief valve on the cover plate of the press regulating valve and the proportional valve to achieve precise control of the slider.

In order to avoid the occurrence of the speed change point A in the open loop control, the two cartridge valves on the master cylinder oil circuit should be started at the end of the fast forward process to complete the initialization of the proportional valve inlet pressure before the start of the punching stage. The proportional valve should also be started for a certain period of time due to the dead band, so that the main spool is located at the 0 position when punching stage is started.

The master cylinder load continues to increase during the pressing of the blank holder, and a load peak appears at the end of the process due to the die closing. The control current of the proportional valve in this region continues to rise, which is helpful in suppressing the speed trough at point C in the open loop control. The pressure difference between the two ends of the proportional valve becomes smaller and the opening of the main spool becomes larger due to the response time of the pressure regulating cartridge, which keeps the flow through the proportional valve relatively stable.

The master cylinder load changes smoothly after the punching process begins, and the proportional valve control current remains constant to maintain the master cylinder speed stable. The master cylinder speed is slowed down due to the load increase during the punching process, which is consistent with the principle of reducing the speed at the beginning of the blanking to increase the life of the die.

The punching force begin to decrease in the middle of the punching process. The slider punching speed starts to rise when the proportional valve control current is constant. But the speed rise is limited due to the regulation of the pressure regulating valve.

The proportional valve control current begins to be reduced when the slider reaches the deceleration point. The proportional valve is almost or completely closed when there is a slight distance from the top dead center, and the cartridge valve in the main oil circuit begins to close. The cartridge is closed when the slider reaches the top dead center, and the punching process ends. The position of the deceleration point is determined by the slider speed, the ramp time and the response time of the proportional valve.

The blanking force is related to the amount of the material deformation in the blanking process, and the counter force is basically unchanged. The unloading speed of the blank holder is the only adjustable parameter. The slower speed stabilizes the master cylinder load but causes a waste of energy. The faster speed reduces the energy loss but causes the speed fluctuation of master cylinder.

From the perspective of the optimization of the punching conditions, the unloading of the blank holder force should not be too fast. The ideal situation is that the reduction of the blank holder force is equal to the increase of the blanking force after the die closing, which keeps the load stable from the die closing to the blanking force rising to the maximum, and stabilizes the punching speed. Although some of the energy is consumed, it is worthwhile for the stability of the system speed and accuracy.

The simulation results of the hydraulic control system in the blanking process based on the slider speed control optimization and load optimization are shown in Fig. 18. In the case of the best fit of all the valves, the slider speed is stable and the overshoot of the master cylinder position is less than 0.005 mm.

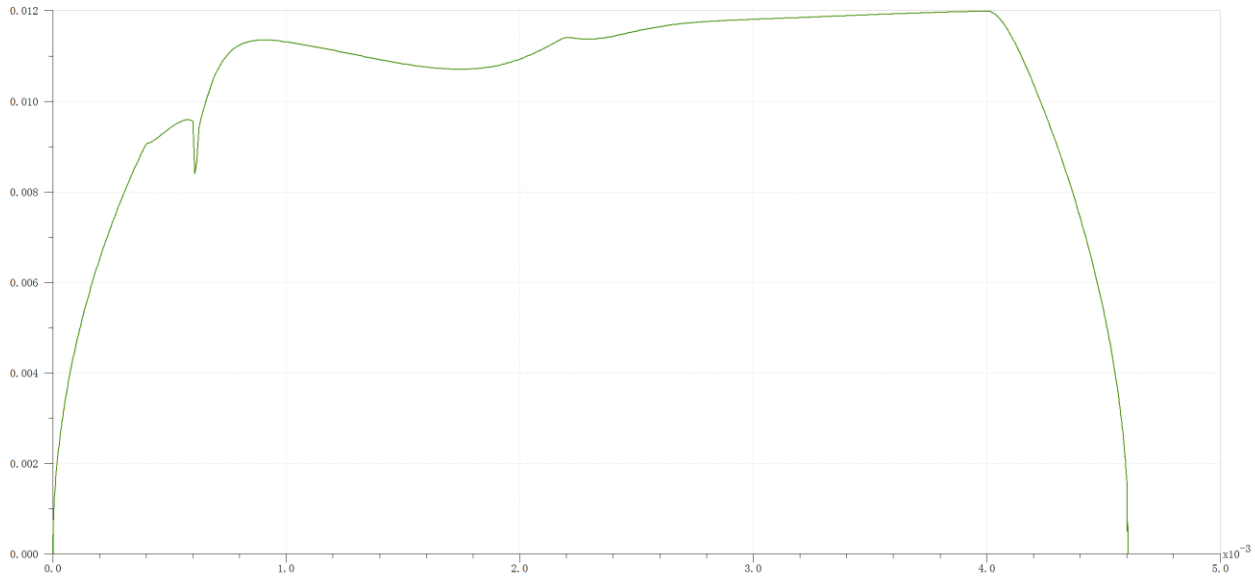

x: Slider displacement (m); y: Slider velocity (m/s).

Fig. 18. Speed curve of the master cylinder with the open-loop optimal control.

The changes of the corresponding force and master cylinder load are shown in Fig. 19, which is moderate compared with the load without optimization, and is conducive to the stability of the slider speed.

The automatic optimization algorithm is based on the basic control system. The algorithm flow chart is shown in Fig. 20.

Data acquisition: collecting and recording the displacement curve of the master cylinder, the pressure time curve of the counter cylinder and the blank holder, the action time of the control current and the spool position data of each valve.

Data analysis: calculate the positions of the speed change points and the maximum blanking force point through integrating the displacement time curve of the master cylinder.

Optimization strategy generation: building a strategy based on the location and timing of velocity change points using theoretical and practical data through the neural network.

Execution or non-execution: deciding whether to execute the optimization strategy based on the current machine conditions and machined parts quality.

Local optimum calculation: finding the optimal set of control parameters through multiple iterations.

Stability analysis: analyzing the variation of all working parameters in each blanking to find the trend of parameters changing as soon as possible and adjust them in time.

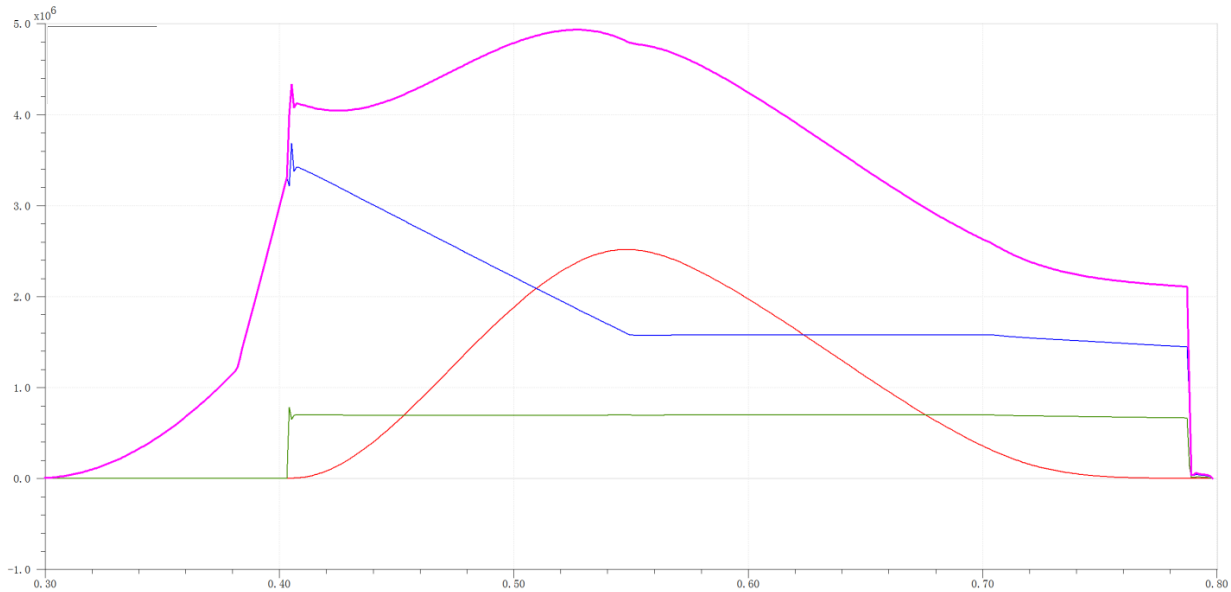

x: Time (s); y: Cutting force (red) (N), counter force (green) (N), blank holder force (blue) (N), total load of the master cylinder (magenta) (N).

Fig. 19. System load changes after the optimization.

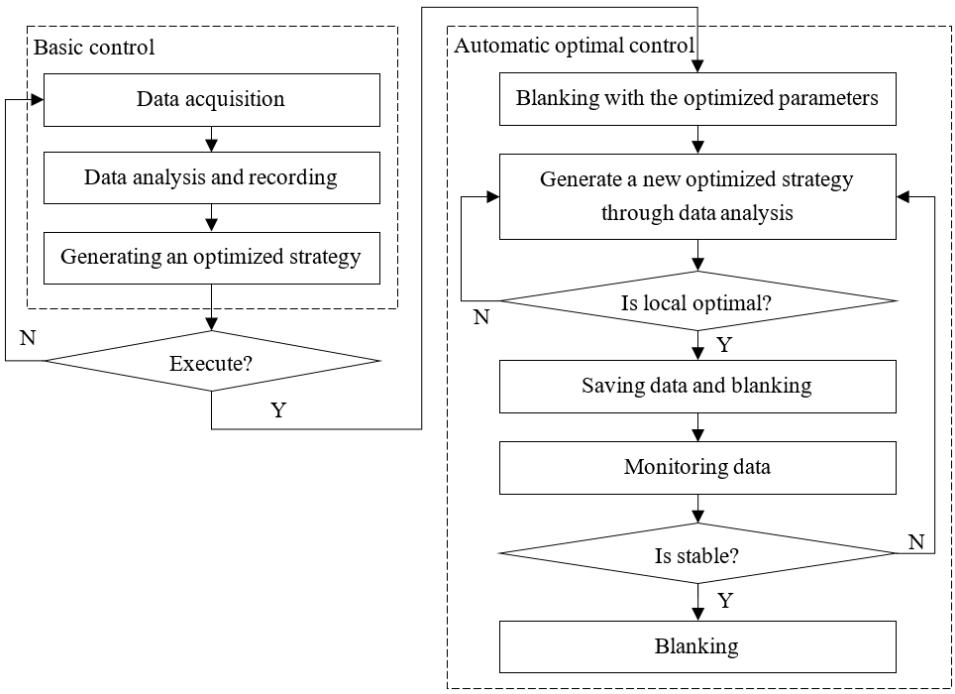

Fig. 20. Flow chart of the automatic optimization algorithm of the control system.

The basic control system is active prior to the optimizing control, and the data is recorded and analyzed to calculate the corresponding optimizing control methods. After starting the optimizing control, the control system determines and corrects the optimal control parameters through multiple

tests, and the parameters will be continuously monitored during the subsequent processing for processing of anomalies timely.

Summary. In this paper, taking the control strategy of the hydraulic system in the blanking and punching stage as the research object, the guiding principle of the control strategy is studied. The system performance of the open - loop control and the closed - loop control and the factors influencing the change point of the component characteristic curve are analyzed, and the reference indexes of the control mode are put forward. The optimizing control algorithm of the process is studied at last.

(1) According to the change of the load in the fine blanking process and the configuration of the hydraulic system, it is appropriate to adopt the open loop control mode in the blanking phase.

(2) The load of the main cylinder changes smoothly through the load and speed control optimization, which is conducive to the stability of the slider speed.

(3) The controllability of the hydraulic system will be improved if damping is used to mitigate the possible impact according to the characteristics of the system load changes.

Acknowledgements

The authors gratefully acknowledge the financial support from the Natural Science Foundation of China (Grant number: 51375438).

References

[1] T. Schwarzgruber, T. E. Passenbrunner, L. Re. Control design for a multi input single output hydraulic cylinder system. 19th IFAC World Congress, Cape Town, South Africa, August 24-29, 2014

[2] W. Shen, J. Jiang, X. Su, H. R. Karimi. Control strategy analysis of the hydraulic hybrid excavator. Journal of the Franklin Institute 352(2015) 541-561

[3] K. Baghestan, S. M. Rezaei, H. A. Talebi, M. Zareinejad. An energy-saving nonlinear position control strategy for electro-hydraulic servo systems. ISA Transactions 59(2015) 268-279

[4] W. Ding, H. Deng, Y. Xia, X. Duan. Tracking control of electro-hydraulic servo multi-closed-chain mechanisms with the use of an approximate nonlinear internal model. Control Engineering Practice 58 (2017) 225- 241

[5] L. S. Coelho, M. A. B. Cunha. Adaptive cascade control of a hydraulic actuator with an adaptive dead-zone compensation and optimization based on evolutionary algorithms. Expert Systems with Applications 38 (2011) 12262–12269

[6] N. M. Tri, D. N. C. Nam, H. G. Park, K. K. Ahn. Trajectory control of an electro hydraulic actuator using an iterative backstepping control scheme. Mechatronics 29 (2015) 96–102

[7] C. Jia, X. Shan, Y. Cui, T. Bai, F. Cui. Modeling and simulation of hydraulic roll bending system based on CMAC neural network and PID coupling control strategy. Journal of Iron and Steel Research, International 2013, 20(10): 17-22

[8] G. Shen, Z. Zhu, J. Zhao, W. Zhu, Y. Tang, X. Li. Real-time tracking control of electro-hydraulic force servo systems using offline feed back control and adaptive control. ISA Transactions 67 (2017), 356-370

[9] P. Chalupa, J. Novák. Modeling and model predictive control of a nonlinear hydraulic system. Computers and Mathematics with Applications 66 (2013), 155–164

[10] Y. Ye, C. Yin, Y. Gong, J. Zhou. Position control of nonlinear hydraulic system using an improved PSO based PID controller. Mechanical Systems and Signal Processing 83 (2017), 241–259

[11] R. Li, J. Luo, C. Sun, S. Liu. Analysis of Electro-hydraulic Proportional Speed Control System on Conveyer. Procedia Engineering 31 (2012), 1185 – 1193

[12] C. Du, A. R. Plummer, D. N. Johnston. Performance analysis of a new energy-efficient variable supply pressure electro-hydraulic motion control method. Control Engineering Practice 60 (2017), 87–98

[13] K. M. Elbayomy, Z. Jiao, H. Zhang. PID Controller Optimization by GA and Its Performances on the Electro-hydraulic Servo Control System. Chinese Journal of Aeronautics 21(2008), 378-384

[14] B. N. Muhammad, S. Wang. Optimization Based on Convergence Velocity and Reliability for Hydraulic Servo System. Chinese Journal of Aeronautics 22(2009), 407-412

[15] H. Cao, H. Guo. Optimization of PID Parameters of Hydraulic System of Elevating Wheelchair Based on AMESim. Procedia Engineering 15 (2011), 3710 – 3714

[16] J. Zheng, S. Zhao, S. Wei. Application of self-tuning fuzzy PID controller for a SRM direct drive volume control hydraulic press. Control Engineering Practice 17 (2009), 1398–1404.